

Electronic Supplementary Information

Magnetic investigations of monocrystalline $[\text{Co}(\text{NCS})_2(\text{L})_2]_n$: new insights into single-chain relaxations

Magdalena Ceglarska, Michael Böhme, Tristan Neumann, Winfried Plass, Christian Näther, and Michał Rams

1 – $[\text{Co}(\text{NCS})_2(4\text{-}(3\text{-phenylpropyl})\text{pyridine})_2]_n$

1-Cd – $[\text{Co}_x\text{Cd}_{1-x}(\text{NCS})_2(4\text{-}(3\text{-phenylpropyl})\text{pyridine})_2]_n$

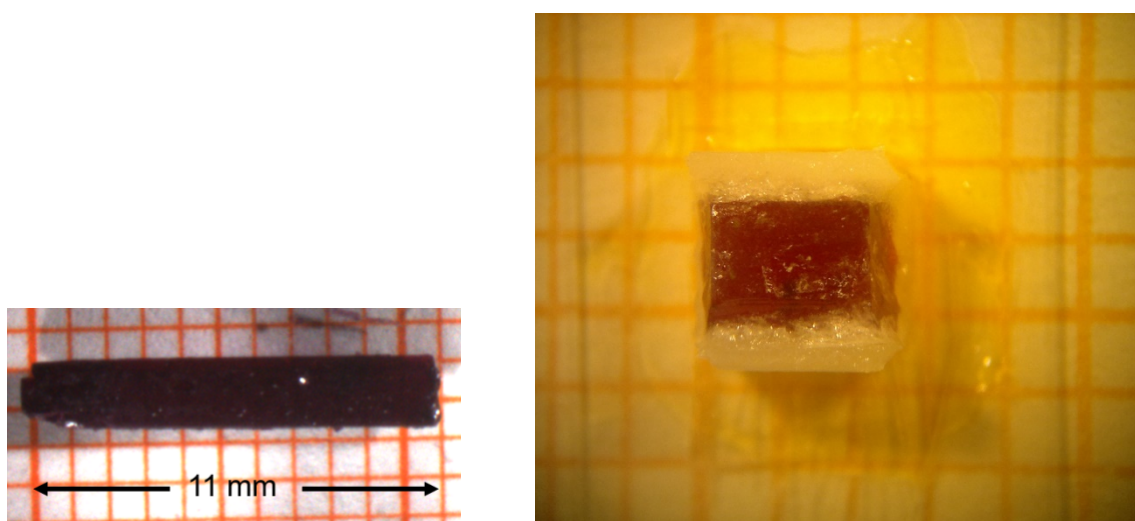


Figure S1. The photos of a single crystal sample of **1**. Left: the whole single crystal. Right: a fragment cut for magnetic measurements, 5.37 mg. The crystal is glued to the holder made of delrin by small amount of Eicosane.

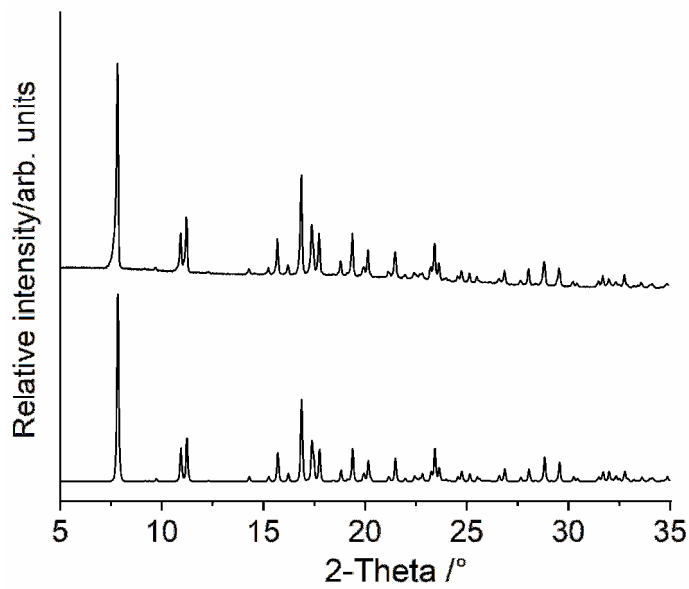


Figure S2a. Experimental (top) and calculated powder pattern (bottom) for **1-Cd** measured with Cu K α radiation. Please note: The crystal structure reported in literature was measured at low temperatures. Therefore, for the calculation of the PXRD pattern the unit cell parameters obtained from a Pawley fit of a powder pattern of to Co compound measured at room-temperature were used.

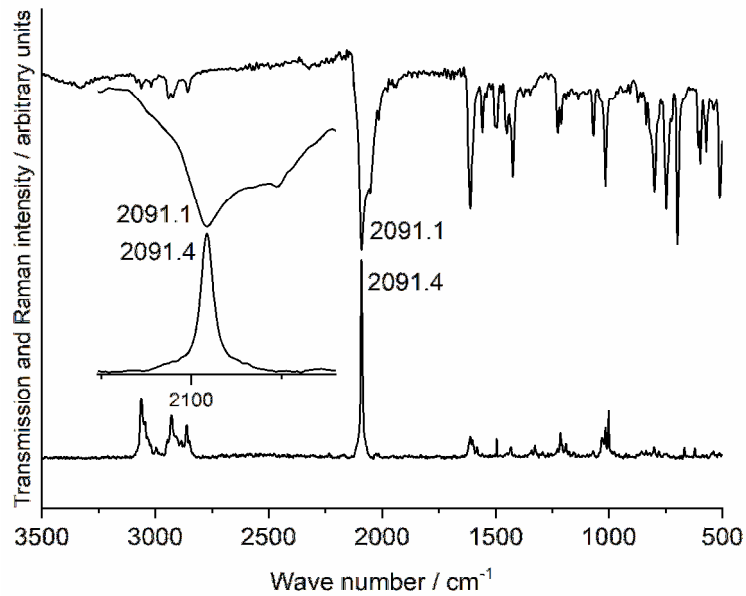


Figure S2b. IR (top) and Raman spectra (bottom) of **1-Cd** ($x = 0.013$). Given are the values of the CN stretching vibration and the inset shows an enlargement of this region. The spectra are very close to that of the pure Cd compound.

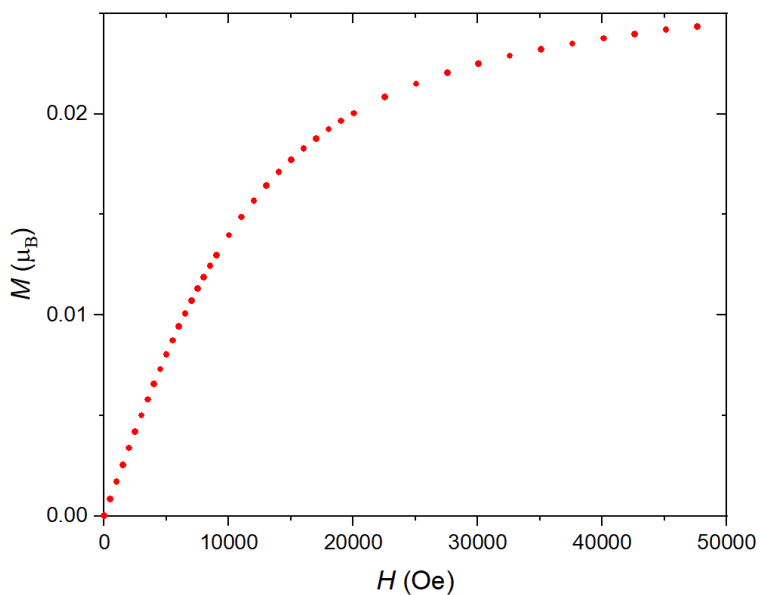


Figure S3. The magnetization curve for **1-Cd** measured at 2 K. The content of Co(II) ions, x , estimated on the basis of comparison of the values of magnetization in 50 kOe for **1-Cd** including diamagnetic corrections and **1** (see Figure 6 in ref. [S1]) and is in agreement with the value from AAS (0.013).

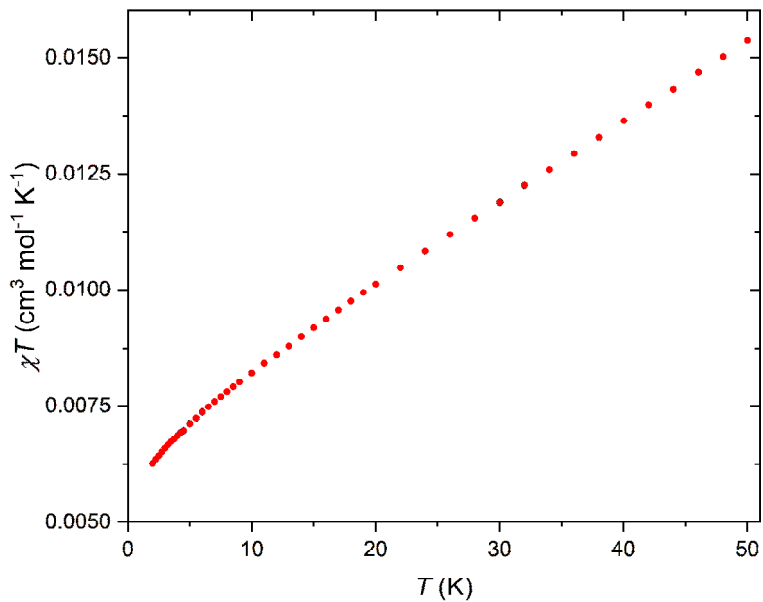


Figure S4. The magnetic susceptibility for **1-Cd** ($x = 0.013$), measured at 100 Oe. The almost linear decrease of χT with decreasing temperature means that Co moments do not interact, i.e. are well diluted. Any presence of **1** would manifest as increase around 3.3 K.

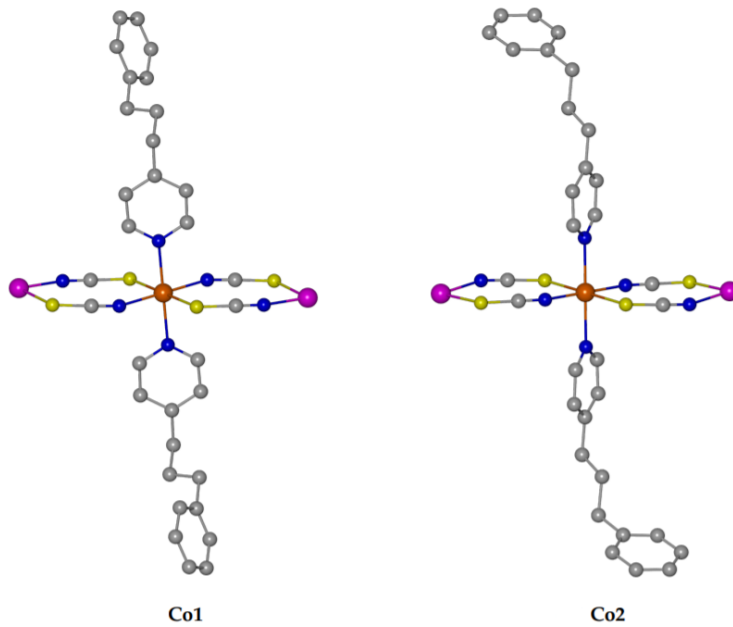


Figure S5. *Ab initio* computational models for **1** (Co – orange; Zn – pink). Hydrogen atoms have been omitted for clarity.

Table S1. Relative CASSCF and CASPT2 energies (in cm⁻¹) of all quartet and the nine lowest doublet states for the mononuclear cobalt(II) computational models (Co1 and Co2) for **1**.

| 2S + 1 | Term | Subterm | Co1 CASSCF | Co1 CASPT2 | Co2 CASSCF | Co2 CASPT2 |
|--------|----------------|------------------------------|---------------|---------------|---------------|---------------|
| 4 | ⁴ F | ⁴ T _{1g} | 0 | 0 | 0 | 0 |
| | | | 505 | 619 | 669 | 588 |
| | | | 1114 | 1051 | 1131 | 1155 |
| | | ⁴ T _{2g} | 5606 | 6668 | 5308 | 5590 |
| | | | 7862 | 9033 | 7807 | 7916 |
| | ⁴ P | ⁴ A _{2g} | 8489 | 9554 | 8841 | 8936 |
| | | | 15471 | 17666 | 15445 | 15850 |
| | | | 21170 | 18651 | 21398 | 21488 |
| | | ⁴ T _{1g} | 22865 | 20756 | 22703 | 22696 |
| | | | 25961 | 23765 | 26183 | 26529 |
| 2 | ² G | | 12118 | 9476 | 11999 | 9362 |
| | | | 15870 | 13141 | 16225 | 13538 |
| | | | 18060 | 15956 | 17599 | 15639 |
| | | | 18591 | 16510 | 18508 | 16467 |
| | | | 19295 | 16733 | 19375 | 16847 |
| | | | 19955 | 17261 | 20011 | 17329 |
| | | | 20861 | 18210 | 20951 | 18312 |
| | | | 21342 | 18510 | 21385 | 18624 |
| | | | 24321 | 16534 | 24305 | 20847 |

Table S2. Relative RASSI-SO energies (in cm^{-1}) of the ${}^4\text{T}_{1g}$ ground state for the mononuclear Co(II) computational models (Co1 and Co2) for **1**.

| Kramers doublet | Co1 | Co2 |
|-----------------|------|------|
| 1 | 0 | 0 |
| 2 | 161 | 140 |
| 3 | 753 | 823 |
| 4 | 1007 | 1081 |
| 5 | 1403 | 1393 |
| 6 | 1508 | 1525 |

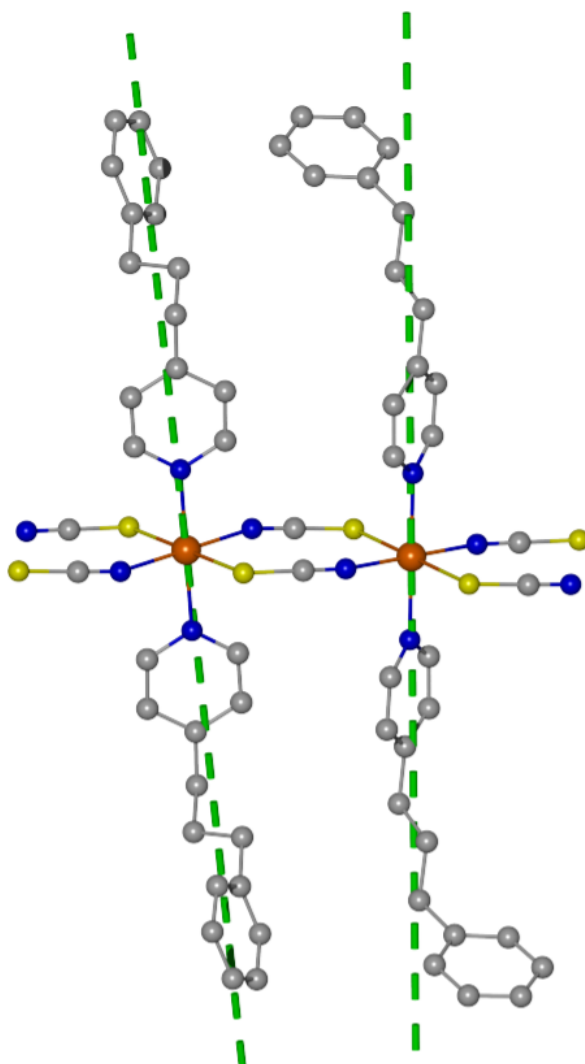


Figure S6. *Ab initio* calculated easy-axes of magnetization ($S_{\text{eff}} = 1/2$) of the ground state Kramers doublet for the individual centers Co1 (left) and Co2 (right) projected onto the smallest repeating sequence of the periodic chain for **1** (angle between the axes: 9.3°). Hydrogen atoms have been omitted for clarity.

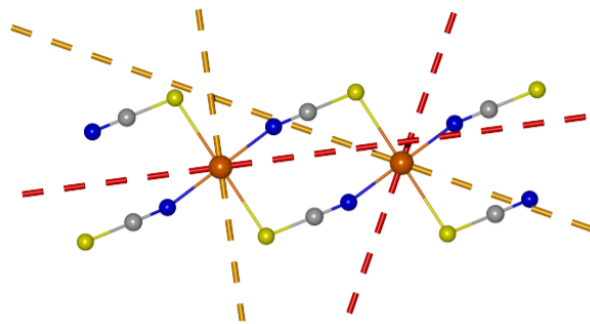


Figure S7. *Ab initio* calculated hard-axes of magnetization ($S_{eff} = 1/2$; red dashed line: g_x ; orange dashed line: g_y) of the ground state Kramers doublet for the individual centers Co1 (left) and Co2 (right) from a top view for **1**. Apical 4-(3-phenylpropyl)pyridine ligands have been omitted for clarity.

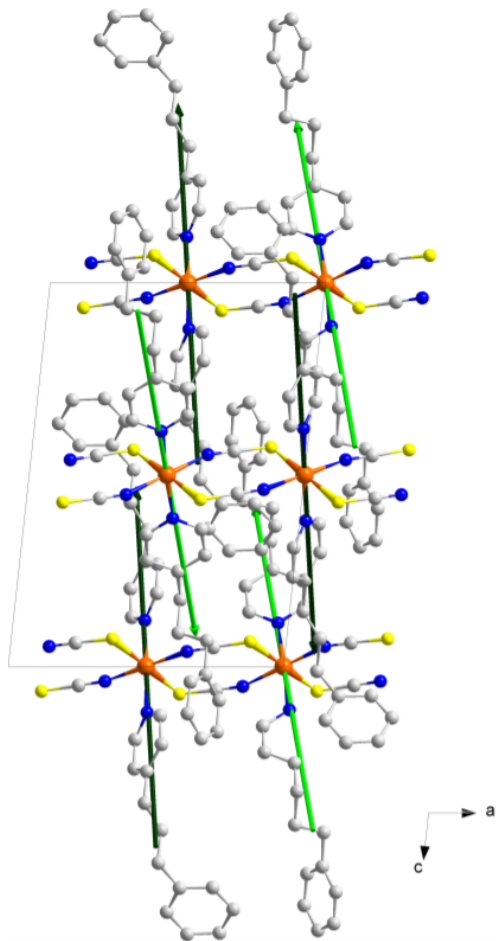


Figure S8. *Ab initio* calculated easy-axes of magnetization ($S_{eff} = 1/2$) of the ground state Kramers doublet for the individual centers Co1 (green) and Co2 (dark green) projected onto the periodic chain structure of **1**. View along \vec{b} .

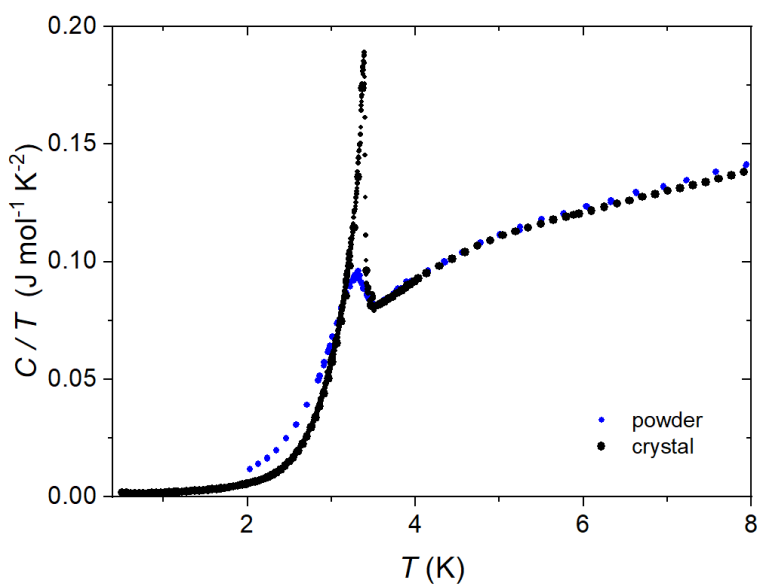


Figure S9. Temperature dependence of the specific heat, C , presented as C/T for a powder and single crystal samples of **1** at $H_{DC} = 0$ Oe.

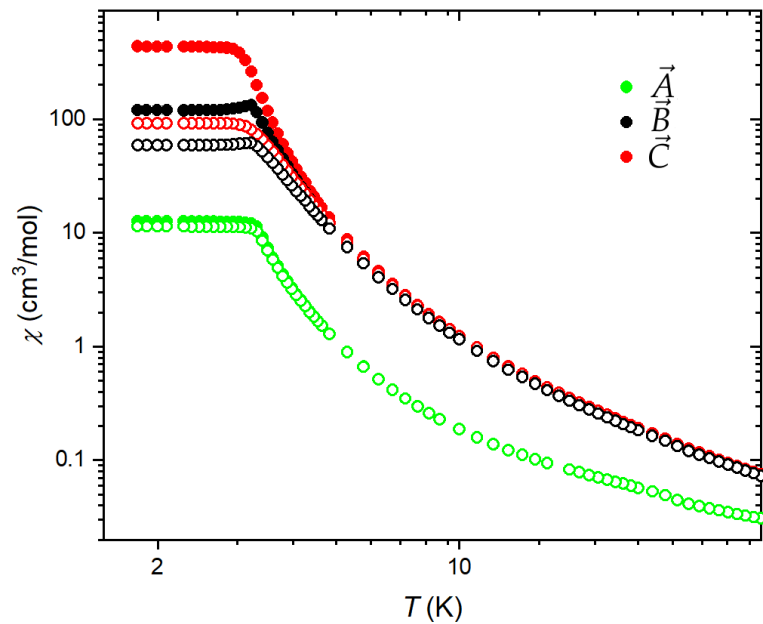


Figure S10. Magnetic susceptibility, χ , measured at $H_{dc} = 100$ Oe for **1** along 3 perpendicular crystallographic directions. Open circles – data as measured, full circles – data corrected for magnetization.^[S3]

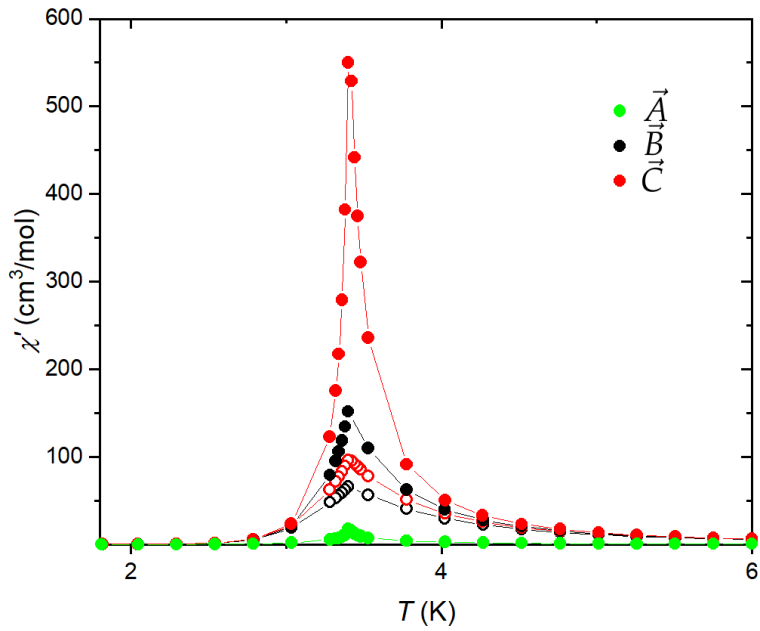


Figure S11. Ac magnetic susceptibility, χ' , measured at $H_{dc} = 0$ Oe, $H_{ac} = 3$ Oe, $f = 10$ Hz for 1 along 3 perpendicular crystallographic directions. Open circles – data as measured, full circles – data corrected for demagnetization.^[S2] The lines are to guide the eye. The demagnetization was included assuming spherical shape of the sample. \vec{A} , \vec{B} , \vec{C} directions are defined in the main text.

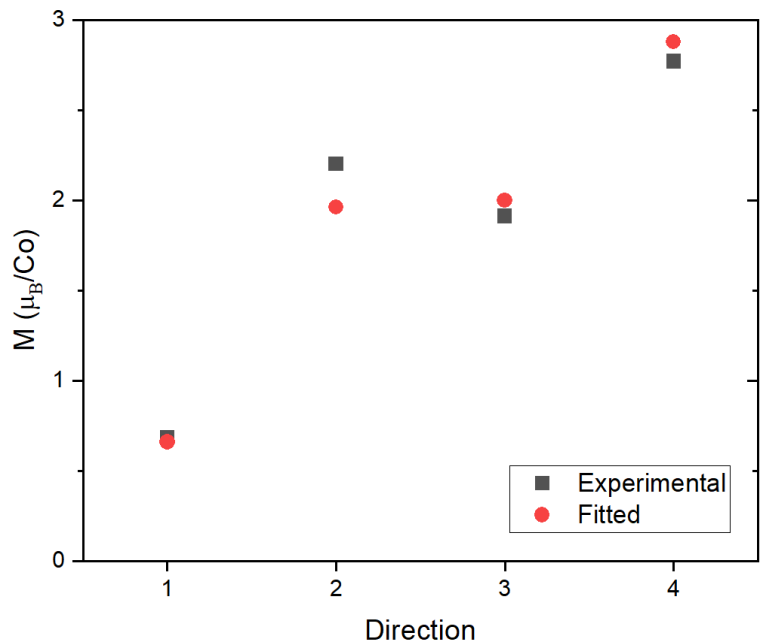


Figure S12. The values of saturation magnetization determined for 4 different directions (1: \vec{A} , 2: \vec{B} , 3: \vec{C} , 4: crystal easy axis) experimentally and fitted.

The conversion of crystallographic coordinates (x, y, z) to Cartesian coordinates (x_c, y_c, z_c) was done using the following equation:

$$\begin{pmatrix} x_c \\ y_c \\ z_c \end{pmatrix} = \begin{pmatrix} a & 0 & a \cdot \cos \beta \\ 0 & b & 0 \\ 0 & 0 & c \cdot \sin \beta \end{pmatrix} \begin{pmatrix} x \\ y \\ z \end{pmatrix} = \begin{pmatrix} 11.27740 & 0 & -1.71896 \\ 0 & 16.03430 & 0 \\ 0 & 0 & 15.72110 \end{pmatrix} \begin{pmatrix} x \\ y \\ z \end{pmatrix}$$

a, b, c, β – unit cell parameters

Easy axis vector in Cartesian coordinates for the first chain in a unit cell:

$$\vec{a}_1 = (M_{xc}, M_{yc}, M_{zc});$$

The easy axis of a second chain in a unit cell is related to the first one by the C_2 symmetry represented by a matrix:

$$C_2 = \begin{pmatrix} -1 & 0 & 0 \\ 0 & 1 & 0 \\ 0 & 0 & -1 \end{pmatrix};$$

According to that, the easy axis vector for the second chain in a unit cell is:

$$\vec{a}_2 = (-M_{xc}, M_{yc}, -M_{zc}).$$

The function used for fitting:

$$\chi^2 = (M_A - F_A)^2 + (M_B - F_B)^2 + (M_C - F_C)^2 + (M_{ea} - F_{ea})^2,$$

where:

M_A, M_B, M_C, M_{ea} – values of magnetization determined experimentally for directions $\vec{A}, \vec{B}, \vec{C}$ and easy axis, respectively, at 2 K and 2 kOe;

F_A, F_B, F_C – projections of the easy axes vectors on the $\vec{A}, \vec{B}, \vec{C}$ directions:

$$F_A = \frac{1}{2}(|\vec{a}_1 \cdot \vec{A}| + |\vec{a}_2 \cdot \vec{A}|)$$

$$F_B = \frac{1}{2}(|\vec{a}_1 \cdot \vec{B}| + |\vec{a}_2 \cdot \vec{B}|)$$

$$F_C = \frac{1}{2}(|\vec{a}_1 \cdot \vec{C}| + |\vec{a}_2 \cdot \vec{C}|)$$

F_{ea} takes the maximal value from: $||(\vec{a}_1 + \vec{a}_2)/2||$ or $||(\vec{a}_1 - \vec{a}_2)/2||$.

To write the magnetic moment in spherical coordinates (M, θ_M, ϕ_M) , conversion of Cartesian coordinates (M_{xc}, M_{yc}, M_{zc}) was done using the following set of equations:

$$\begin{cases} M = \sqrt{M_{xc}^2 + M_{yc}^2 + M_{zc}^2} \\ \theta_M = \cos^{-1}\left(\frac{M_{zc}}{\sqrt{M_{xc}^2 + M_{yc}^2 + M_{zc}^2}}\right) \\ \phi_M = \tan^{-1}\left(\frac{M_{yc}}{M_{xc}}\right) \end{cases}$$

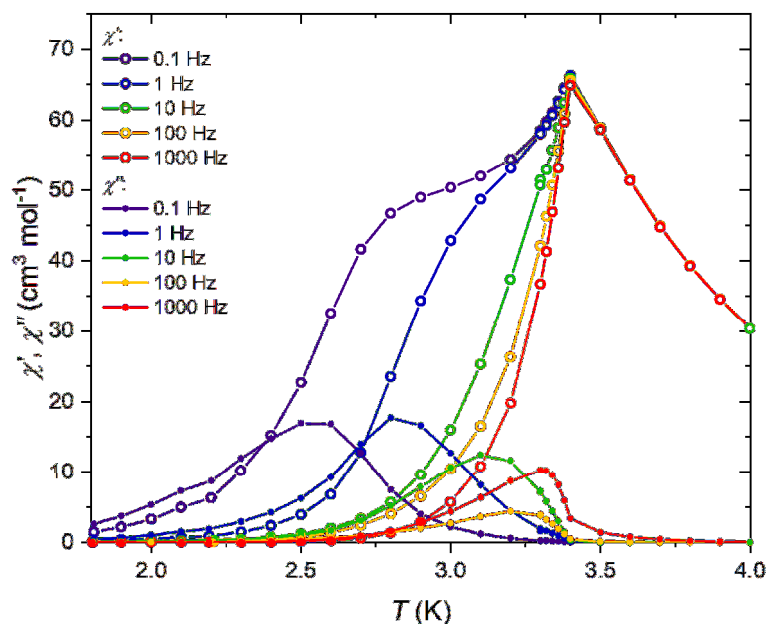


Figure S13. The temperature dependence of ac magnetic susceptibility measured for **1** at $H_{dc} = 0$ and $H_{ac} = 3$ Oe along the $\vec{B} = \vec{b}^* - \vec{c}^*$ direction.

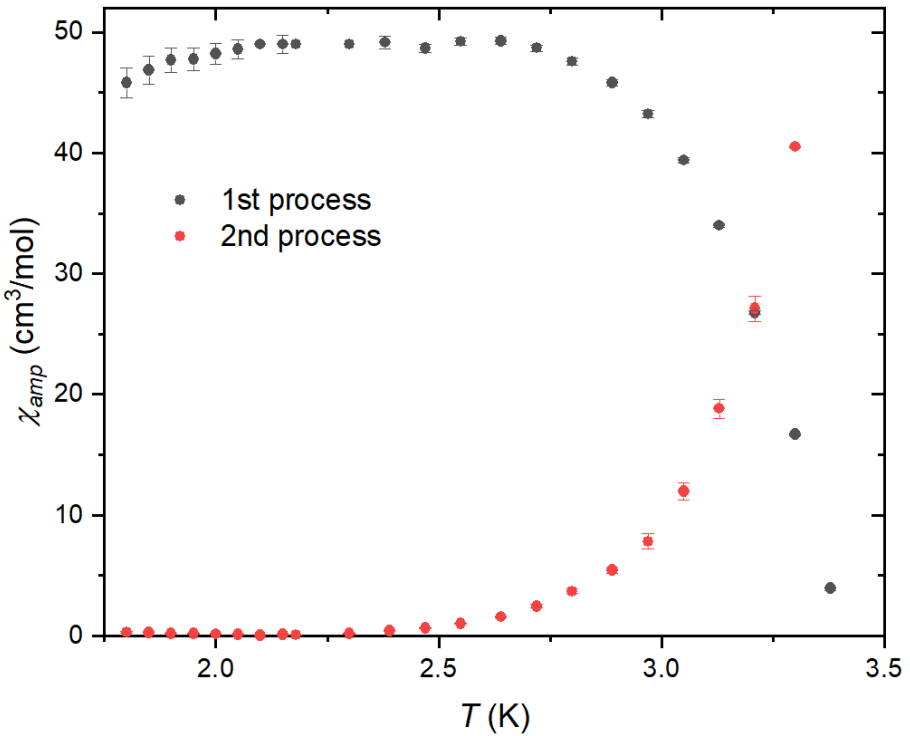


Figure S14. The amplitude of the magnetic susceptibility obtained from the fitting of the Cole-Cole model for both relaxation processes for **1**.

The analysis of the ac magnetic susceptibility was done by using the single-mode Cole-Cole model:

$$\chi_{AC} = \chi_0 + \frac{\chi_1}{1 + (i\omega\tau_1)^{1-\alpha_1}}$$

or double-mode Cole-Cole model:

$$\chi_{AC} = \chi_0 + \frac{\chi_1}{1 + (i\omega\tau_1)^{1-\alpha_1}} + \frac{\chi_2}{1 + (i\omega\tau_2)^{1-\alpha_2}}$$

(χ_0 - the adiabatic limit of the magnetic susceptibility, χ_1 and χ_2 - the amplitudes of the processes, τ - a relaxation time, α - parameter describing the dispersion of the relaxation times). [S4]

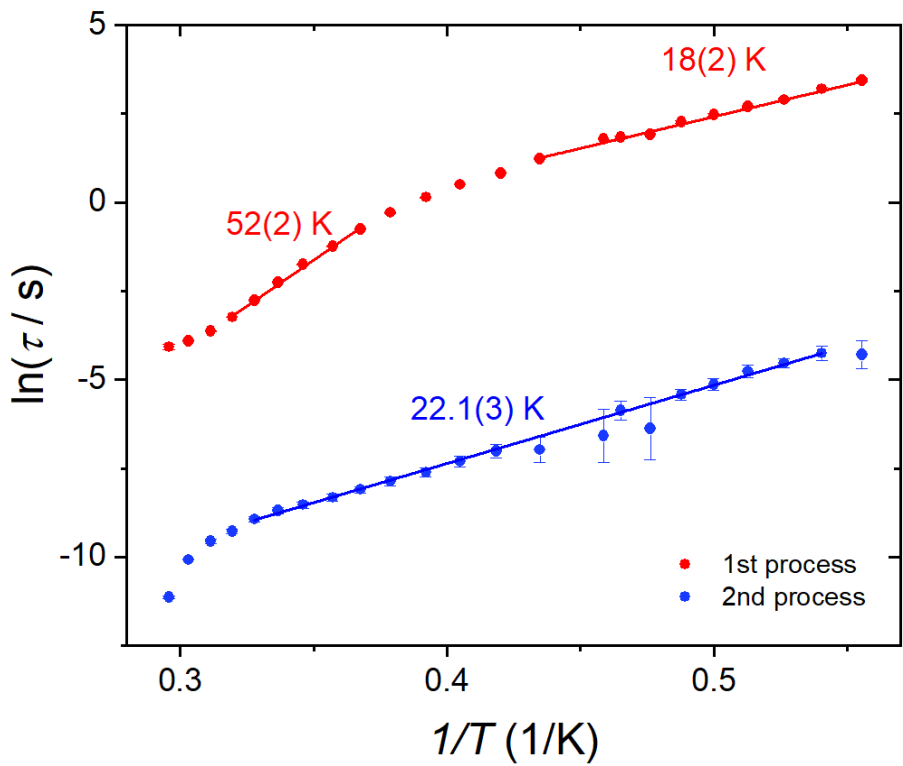


Figure S15. The relaxation times of 1. Red points – SCM relaxation process. Blue points - the faster relaxation process. Lines – the fits of the Arrhenius law.

Table S3. Parameters obtained from fitting the double-mode Cole-Cole model to the ac magnetic susceptibility, χ' and χ'' , vs. frequency, f , dependence measured for **1** at $H_{dc} = 0$ Oe from 1.8 to 3.38 K. The first process, assigned with lower index 1, is the SCM relaxation process, the second process, assigned with lower index 2, is the faster relaxation process (spin wave excitations). (fixed parameters do not have any uncertainty given)

| T | χ_0 | χ_1 | χ_2 | τ_1 | τ_2 | α_1 | α_2 |
|----------|---------------------------|---------------------------|---------------------------|-------------|----------------------------|------------|------------|
| K | cm³/mol | cm³/mol | cm³/mol | s | s | - | - |
| 1.8 | 0.104(35) | 45.8(1.3) | 0.308(65) | 31.4(1.6) | 0.0137(54) | 0.2221(63) | 0.23(17) |
| 1.85 | 0.054(45) | 46.9(1.2) | 0.269(16) | 24.6(1.1) | 0.0141(30) | 0.2239(66) | 0.32981 |
| 1.9 | 0.05387 | 47.7(99) | 0.205(14) | 18.18(73) | 0.0107(14) | 0.2253(61) | 0.272(50) |
| 1.95 | 0.05387 | 47.74(95) | 0.179(18) | 14.87(57) | 0.0084(15) | 0.2213(66) | 0.270(66) |
| 2 | 0.05387 | 48.20(86) | 0.140(15) | 11.91(42) | 0.0059(11) | 0.2205(68) | 0.205(80) |
| 2.05 | 0.05387 | 48.58(80) | 0.116(12) | 9.63(32) | 0.00442(70) | 0.2209(70) | 0.090(91) |
| 2.1 | 0.046(20) | 49 | 0.060(23) | 6.813(34) | 0.0017(15) | 0.1797(19) | 0.03552 |
| 2.15 | 0.05387 | 49.01(77) | 0.117(14) | 6.31(21) | 0.00283(76) | 0.2226(81) | 0.03552 |
| 2.18 | 0.042(22) | 49 | 0.075(25) | 5.922(27) | 0.0014(11) | 0.1860(18) | 0.03552 |
| 2.3 | 0.035(30) | 49 | 0.204(33) | 3.422(13) | 9.4(3.4)·10 ⁻⁴ | 0.1737(28) | 0.03552 |
| 2.38 | 0.05387 | 49.14(52) | - | 2.274(56) | - | 0.2206(81) | - |
| 2.39 | 0.046(32) | - | 0.392(35) | - | 8.9(1.8)·10 ⁻⁴ | - | 0.03552 |
| 2.47 | 0.054(43) | 48.65(36) | 0.638(46) | 1.664(22) | 6.7(1.1)·10 ⁻⁴ | 0.1852(29) | 0.03552 |
| 2.55 | 0.051(59) | 49.24(31) | 1.033(62) | 1.149(13) | 4.92(60)·10 ⁻⁴ | 0.1913(30) | 0.03552 |
| 2.64 | 0.076(92) | 49.28(30) | 1.588(93) | 0.7466(79) | 3.82(44)·10 ⁻⁴ | 0.1967(35) | 0.03552 |
| 2.72 | 0.11(13) | 48.68(26) | 2.46(13) | 0.4681(44) | 3.02(29)·10 ⁻⁴ | 0.1990(36) | 0.03552 |
| 2.8 | 0.18(20) | 47.58(28) | 3.70(19) | 0.2872(31) | 2.42(23)·10 ⁻⁴ | 0.1997(46) | 0.03552 |
| 2.89 | 0.35(29) | 45.81(29) | 5.44(28) | 0.1743(21) | 1.97(18)·10 ⁻⁴ | 0.1978(55) | 0.03552 |
| 2.97 | 0.82(58) | 43.21(29) | 7.82(65) | 0.1043(12) | 1.67(17)·10 ⁻⁴ | 0.1888(59) | 0.036(50) |
| 3.05 | 1.01(65) | 39.38(21) | 11.95(72) | 0.06258(56) | 1.30(11)·10 ⁻⁴ | 0.1721(47) | 0.091(32) |
| 3.13 | 0.54(72) | 33.99(15) | 18.83(79) | 0.03908(27) | 9.33(58)·10 ⁻⁵ | 0.1516(36) | 0.152(19) |
| 3.21 | 1.4(1.0) | 26.76(14) | 27.1(1.1) | 0.02631(21) | 7.01(43)·10 ⁻⁵ | 0.1393(41) | 0.163(15) |
| 3.3 | 1.40374 | 16.70(11) | 40.526(80) | 0.01988(21) | 4.189(37)·10 ⁻⁵ | 0.1384(55) | 0.1493(54) |
| 3.38 | 1.40374 | 3.92(14) | 59.34(10) | 0.0170(13) | 1.457(44)·10 ⁻⁵ | 0.245(31) | 0.011(13) |

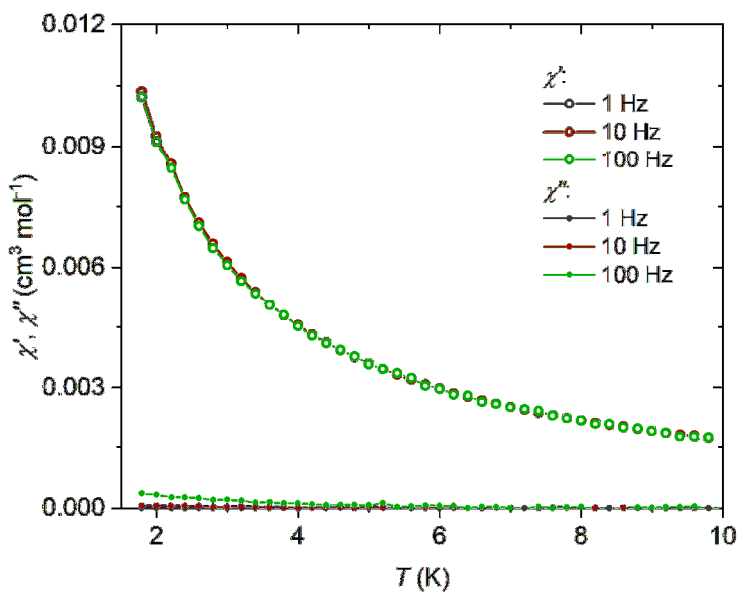


Figure S16. The ac magnetic susceptibility measured for **1-Cd** ($x = 0.013$) at $H_{dc} = 0$ and $H_{ac} = 3$ Oe. No significant difference between the courses of the points indicates good magnetic dilution.

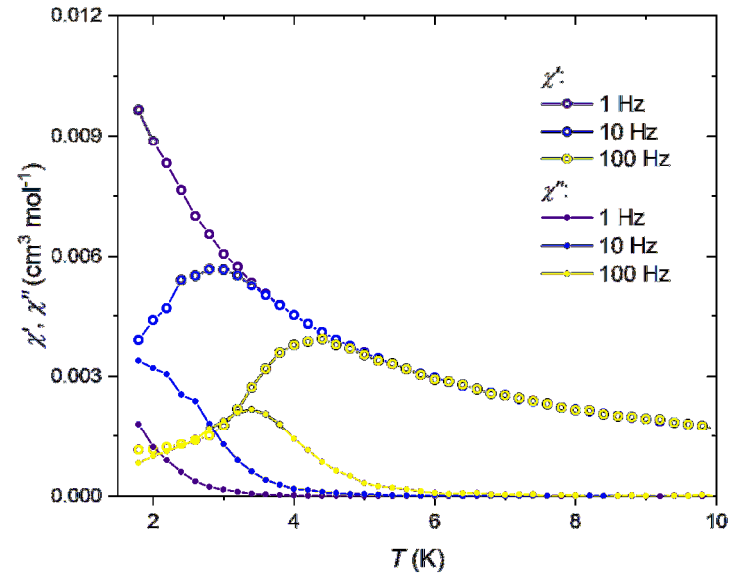


Figure S17. The ac magnetic susceptibility measured for **1-Cd** ($x = 0.013$) at $H_{dc} = 1$ kOe and $H_{ac} = 3$ Oe. The difference for points measured at different frequencies is well visible below 4.5 K.

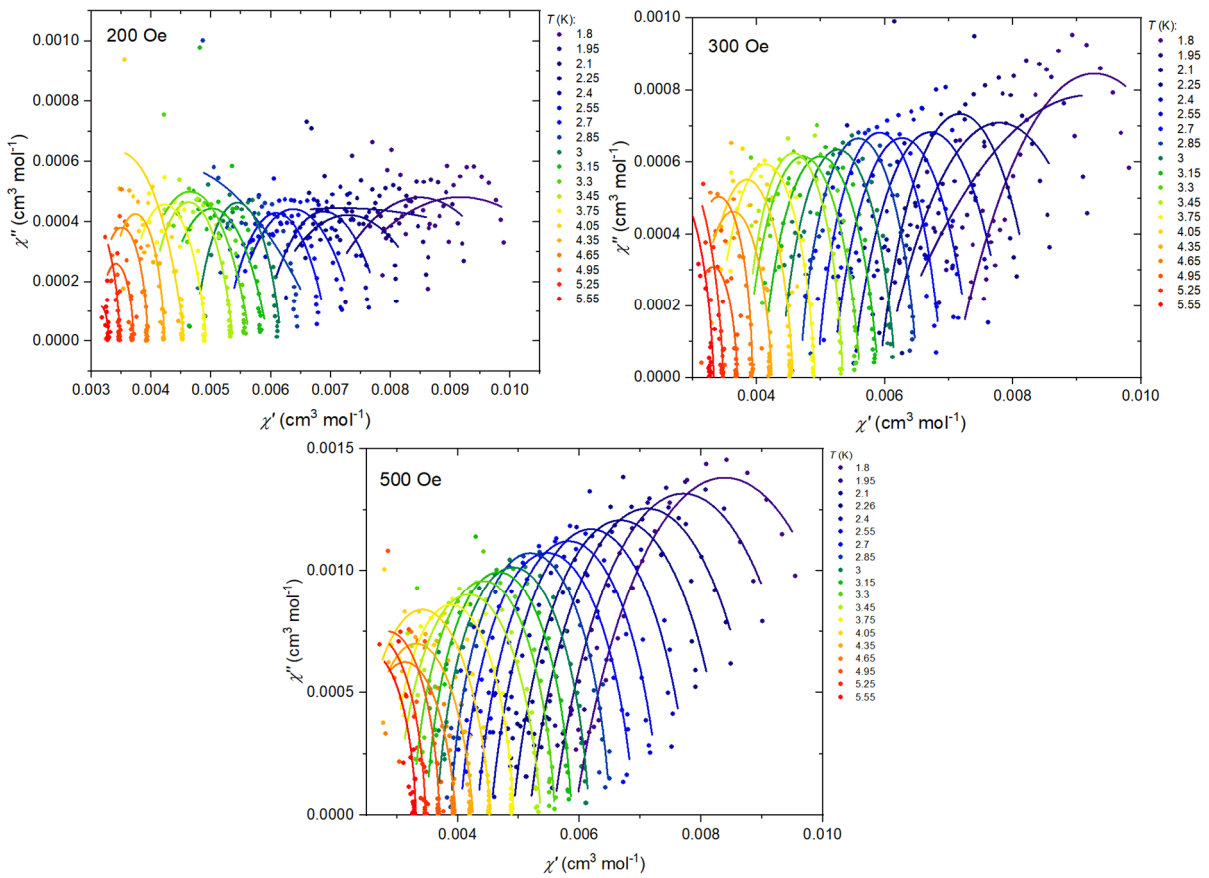


Figure S18. The Argand plots of ac magnetic susceptibility measured at $H_{ac} = 3$ Oe in temperatures below 6 K at 3 different fields (200, 300, 500 Oe) for **1-Cd** ($x = 0.013$). The solid lines are the fits of the single-mode Cole-Cole model.

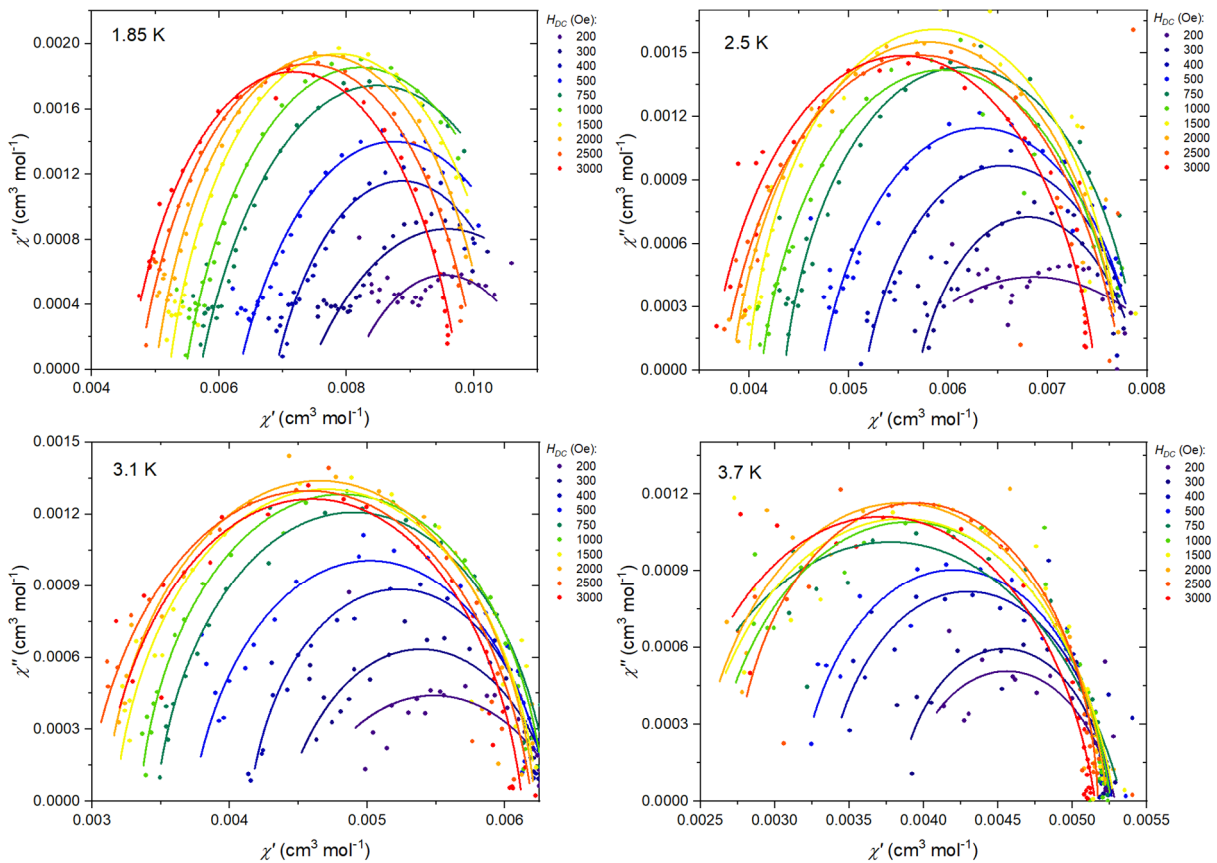


Figure S19. The Argand plot of ac magnetic susceptibility measured at 1.85, 2.5, 3.1 and 3.7 K at $H_{ac} = 3$ Oe and at dc fields up to 3 kOe for **1-Cd** ($x = 0.013$). The solid lines are the fits of the single-mode Cole-Cole model.

Table S4. Parameters obtained from fitting the single-mode Cole-Cole model to the ac magnetic susceptibility, χ' and χ'' , vs. frequency, f , dependence measured for **1-Cd** ($x = 0.013$) at 1.85 K from 400 to 3000 Oe.

| H | χ^0 | χ_1 | τ_1 | α_1 |
|------|------------|-------------|-------------|------------|
| Oe | cm³/mol | cm³/mol | s | - |
| 400 | 0.00689(4) | 0.00397(16) | 0.0373(28) | 0.327(23) |
| 500 | 0.00632(5) | 0.00486(25) | 0.0458(47) | 0.334(27) |
| 750 | 0.00572(4) | 0.00556(23) | 0.0566(43) | 0.287(21) |
| 1000 | 0.00548(4) | 0.00548(21) | 0.0516(33) | 0.243(21) |
| 1500 | 0.00522(5) | 0.00531(17) | 0.0297(14) | 0.197(20) |
| 2000 | 0.00500(5) | 0.00526(12) | 0.01406(48) | 0.194(17) |
| 2500 | 0.00475(4) | 0.00529(79) | 0.00664(16) | 0.215(12) |
| 3000 | 0.00458(4) | 0.00517(6) | 0.00334(6) | 0.2165(84) |

Table S5. Parameters obtained from fitting the single-mode Cole-Cole model to the ac magnetic susceptibility, χ' and χ'' , vs. frequency, f , dependence measured for **1-Cd** ($x = 0.013$) at 2.5 K from 300 to 3000 Oe.

| H | χ_0 | χ_1 | τ_1 | α_1 |
|-----------|---------------------------|---------------------------|-------------|------------|
| Oe | cm³/mol | cm³/mol | s | - |
| 300 | 0.0057(4) | 0.00222(9) | 0.01096(72) | 0.262(28) |
| 400 | 0.00517(5) | 0.00278(12) | 0.01187(79) | 0.225(31) |
| 500 | 0.00472(6) | 0.00320(14) | 0.01233(81) | 0.210(31) |
| 750 | 0.00435(5) | 0.00357(12) | 0.01460(70) | 0.140(25) |
| 1000 | 0.00412(5) | 0.00365(12) | 0.01438(65) | 0.159(23) |
| 1500 | 0.00399(5) | 0.00377(12) | 0.01174(49) | 0.099(24) |
| 2000 | 0.00383(5) | 0.00394(10) | 0.00755(26) | 0.150(18) |
| 2500 | 0.00373(12) | 0.00402(24) | 0.00455(41) | 0.189(44) |
| 3000 | 0.00361(7) | 0.00388(12) | 0.00231(11) | 0.167(23) |

Table S6. Parameters obtained from fitting the single-mode Cole-Cole model to the ac magnetic susceptibility, χ' and χ'' , vs. frequency, f , dependence measured for **1-Cd** ($x = 0.013$) at 3.1 K from 300 to 3000 Oe.

| H | χ_0 | χ_1 | τ_1 | α_1 |
|-----------|---------------------------|---------------------------|-------------|------------|
| Oe | cm³/mol | cm³/mol | s | - |
| 300 | 0.00440(7) | 0.00198(11) | 0.00277(24) | 0.275(38) |
| 400 | 0.00415(3) | 0.00216(5) | 0.00358(12) | 0.127(18) |
| 500 | 0.00373(6) | 0.00259(10) | 0.00333(19) | 0.159(30) |
| 750 | 0.00347(3) | 0.00286(6) | 0.00400(10) | 0.108(15) |
| 1000 | 0.00335(3) | 0.00295(5) | 0.00408(80) | 0.088(12) |
| 1500 | 0.00317(5) | 0.00307(10) | 0.00371(15) | 0.104(23) |
| 2000 | 0.00309(5) | 0.00313(9) | 0.00297(11) | 0.099(21) |
| 2500 | 0.00295(7) | 0.00324(12) | 0.00208(10) | 0.141(26) |
| 3000 | 0.00307(7) | 0.00305(10) | 0.00149(7) | 0.120(24) |

Table S7. Parameters obtained from fitting the single-mode Cole-Cole model to the ac magnetic susceptibility, χ' and χ'' , vs. frequency, f , dependence measured for **1-Cd** ($x = 0.013$) at 3.7 K from 200 to 3000 Oe.

| H | χ_0 | χ_1 | τ_1 | α_1 |
|-----------|---------------------------|---------------------------|-------------|------------|
| Oe | cm³/mol | cm³/mol | s | - |
| 200 | 0.00383(10) | 0.00145(13) | 0.00063(9) | 0.224(53) |
| 300 | 0.00382(6) | 0.00145(8) | 0.00106(8) | 0.124(39) |
| 400 | 0.00333(6) | 0.00194(9) | 0.00104(7) | 0.107(32) |
| 500 | 0.00316(4) | 0.00210(6) | 0.00113(4) | 0.096(18) |
| 750 | 0.0022(3) | 0.00312(23) | 0.00077(13) | 0.266(58) |
| 1000 | 0.00254(8) | 0.00271(11) | 0.00106(6) | 0.138(27) |
| 1500 | 0.0024(2) | 0.00285(17) | 0.00104(9) | 0.160(39) |
| 2000 | 0.00246(7) | 0.00278(11) | 0.00105(5) | 0.111(26) |
| 2500 | 0.00272(6) | 0.00245(9) | 0.00097(5) | 0.033(27) |
| 3000 | 0.0023(2) | 0.00287(15) | 0.00060(5) | 0.160(31) |

Table S8. Parameters obtained from fitting the single-mode Cole-Cole model to the ac magnetic susceptibility, χ' and χ'' , vs. frequency, f , dependence measured for **1-Cd** ($x = 0.013$) at 200 Oe from 1.8 to 5.5 K.

| T | χ_0 | χ_1 | τ_1 | α_1 |
|----------|---------------------------|---------------------------|--------------------------|------------|
| K | cm^{3/mol} | cm^{3/mol} | 10⁻⁴ s | - |
| 1.80 | 0.00656 | 0.00523(59) | 0.017(17) | 0.768(22) |
| 1.95 | 0.00656(27) | 0.00387(75) | 0.0153(76) | 0.690(59) |
| 2.10 | 0.00174(95) | 0.0109(17) | 0.0010(52) | 0.90(16) |
| 2.25 | 0.00566(38) | 0.00327(78) | 0.0058(27) | 0.678(78) |
| 2.40 | 0.00581(11) | 0.00216(21) | 0.0063(12) | 0.514(48) |
| 2.55 | 0.00525(12) | 0.00225(22) | 0.0040(71) | 0.523(46) |
| 2.70 | 0.00521(8) | 0.00176(14) | 0.0040(55) | 0.423(45) |
| 2.85 | 0.00161(31) | 0.005(34) | 0.00003(11) | 0.719(96) |
| 3.00 | 0.00472(5) | 0.00145(8) | 0.00248(23) | 0.277(39) |
| 3.15 | 0.00409(23) | 0.00187(31) | 0.00093(34) | 0.436(81) |
| 3.30 | 0.00365(15) | 0.00201(19) | 0.00056(12) | 0.412(43) |
| 3.45 | 0.00389(6) | 0.00148(73) | 0.00082(7) | 0.284(29) |
| 3.75 | 0.00354(7) | 0.00139(9) | 0.00056(6) | 0.257(35) |
| 4.05 | 0.00239(38) | 0.00217(41) | 0.00014(6) | 0.329(35) |
| 4.35 | 0.00326(10) | 0.0001(2) | 0.00034(5) | 0.076(66) |
| 4.65 | 0.00308(4) | 0.00086(5) | 0.00028(2) | 0.07641 |
| 4.95 | 0.00312(5) | 0.00059(7) | 0.00031(5) | 0.07641 |
| 5.25 | 0.00257(13) | 0.0001(2) | 0.00010(2) | 0.07641 |
| 5.55 | 0.00303(6) | 0.00026(7) | 0.00025(8) | 0.07641 |

Table S9. Parameters obtained from fitting the single-mode Cole-Cole model to the ac magnetic susceptibility, χ' and χ'' , vs. frequency, f , dependence measured for **1-Cd** ($x = 0.013$) at 300 Oe from 1.8 to 5.5 K.

| T | χ_0 | χ_1 | τ_1 | α_1 |
|----------|---------------------------|---------------------------|---------------------------|------------|
| K | cm^{3/mol} | cm^{3/mol} | s | - |
| 1.80 | 0.00705(11) | 0.00445(64) | 0.069(30) | 0.537(50) |
| 2.10 | 0.00597(14) | 0.00365(54) | 0.030(12) | 0.528(63) |
| 2.25 | 0.00591(5) | 0.00253(14) | 0.0182(18) | 0.332(32) |
| 2.40 | 0.00549(7) | 0.00246(19) | 0.0138(20) | 0.355(47) |
| 2.55 | 0.00519(6) | 0.00217(12) | 0.00950(85) | 0.299(37) |
| 2.70 | 0.00494(4) | 0.00195(9) | 0.00727(51) | 0.224(33) |
| 2.85 | 0.00467(3) | 0.00184(6) | 0.00526(25) | 0.203(23) |
| 3.00 | 0.00437(3) | 0.00180(6) | 0.00353(16) | 0.217(21) |
| 3.15 | 0.00409(4) | 0.00182(6) | 0.00255(14) | 0.241(24) |
| 3.30 | 0.00383(7) | 0.00179(10) | 0.00173(15) | 0.232(38) |
| 3.45 | 0.00382(4) | 0.00153(5) | 0.00157(63) | 0.127(21) |
| 3.75 | 0.00336(4) | 0.00155(5) | 7.88(35)·10 ⁻⁴ | 0.167(20) |
| 4.05 | 0.00313(5) | 0.00144(7) | 5.31(39)·10 ⁻⁴ | 0.16715 |
| 4.35 | 0.00303(5) | 0.00121(6) | 3.90(32)·10 ⁻⁴ | 0.16715 |
| 4.65 | 0.00289(8) | 0.00104(9) | 2.68(27)·10 ⁻⁴ | 0.022(40) |
| 4.95 | 0.00295(7) | 0.00008(8) | 2.68(40)·10 ⁻⁴ | 0.1235 |
| 5.25 | 0.00203(42) | 0.00145(44) | 6.9(31)·10 ⁻⁵ | 0.124(69) |
| 5.55 | 0.00203 | 0.00130(46) | 9.1(22)·10 ⁻⁵ | 0.1235 |

Table S10. Parameters obtained from fitting the single-mode Cole-Cole model to the ac magnetic susceptibility, χ' and χ'' , vs. frequency, f , dependence measured for **1-Cd** ($x = 0.013$) at 500 Oe from 1.8 to 5.5 K.

| T | χ_0 | χ_1 | τ_1 | α_1 |
|------|----------------------|----------------------|-------------|------------|
| K | cm ³ /mol | cm ³ /mol | s | - |
| 1.80 | 0.00592(5) | 0.00494(23) | 0.0508(49) | 0.351(23) |
| 1.95 | 0.00557(4) | 0.00428(17) | 0.0375(27) | 0.300(22) |
| 2.10 | 0.00518(4) | 0.00387(13) | 0.0279(15) | 0.267(20) |
| 2.25 | 0.00491(4) | 0.00355(13) | 0.0209(13) | 0.239(24) |
| 2.40 | 0.00455(5) | 0.00329(14) | 0.01517(95) | 0.213(29) |
| 2.55 | 0.00432(5) | 0.00301(13) | 0.01221(75) | 0.185(31) |
| 2.70 | 0.00404(3) | 0.00287(9) | 0.00814(39) | 0.182(24) |
| 2.85 | 0.00388(3) | 0.00263(5) | 0.00630(15) | 0.128(13) |
| 3.00 | 0.00366(5) | 0.00250(10) | 0.00446(25) | 0.133(30) |
| 3.15 | 0.00348(4) | 0.00239(7) | 0.00330(13) | 0.117(21) |
| 3.30 | 0.00326(6) | 0.00234(10) | 0.00234(14) | 0.126(33) |
| 3.45 | 0.00299(6) | 0.00237(10) | 0.00159(9) | 0.173(29) |
| 3.75 | 0.00287(5) | 0.00205(7) | 0.00102(4) | 0.111(21) |
| 4.05 | 0.00230(11) | 0.00224(14) | 0.00047(5) | 0.181(36) |
| 4.35 | 0.00239(6) | 0.00187(8) | 0.00037(3) | 0.18132 |
| 4.65 | 0.00230(9) | 0.00167(10) | 0.00026(3) | 0.18132 |
| 4.95 | 0.00203(4) | 0.00167(35) | 0.00016(5) | 0.070(83) |
| 5.25 | 0.00184(12) | 0.00163(14) | 0.00011(2) | 0.07026 |
| 5.55 | 0.00184 | 0.00147(4) | 0.00011(2) | 0.07026 |

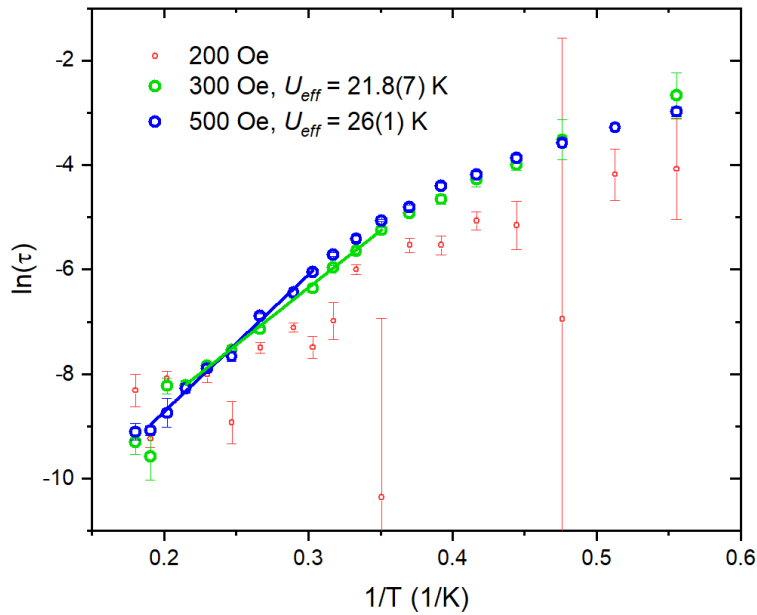


Figure S20. Temperature dependence of the relaxation times for **1-Cd** ($x = 1.3\%$). Solid lines represent a fit of the Arrhenius law describing the Orbach process of relaxation of single spins. The determined effective energy barriers are 21.8(7) K for 300 Oe and 26(1) K for 500 Oe.

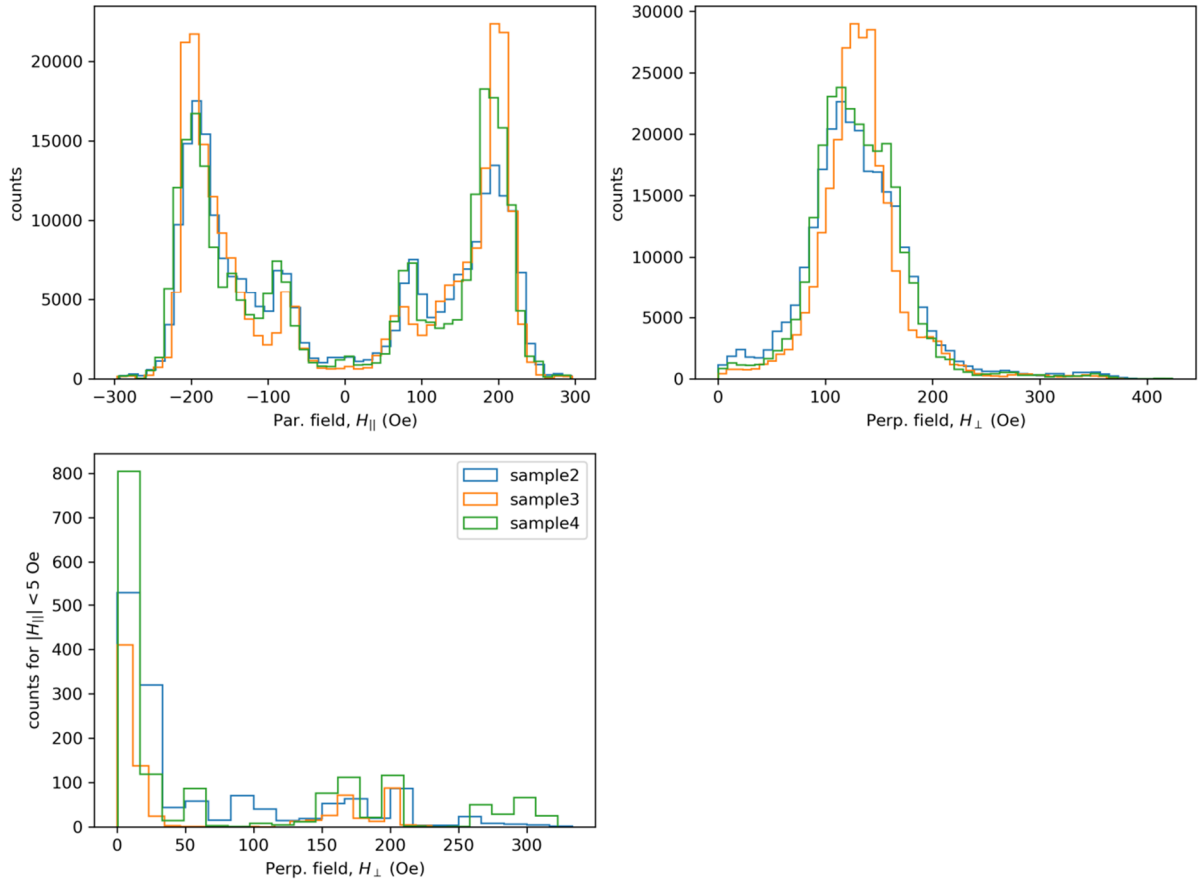


Figure S21. Distribution of dipolar field at Co site obtained from classical Monte-Carlo simulations (see text) for three different domain structures. Top left: Field parallel to easy axis is of order of 200 Oe for most of the spins. Spins at a boundary of the domain experience smaller fields. Top right: Field perpendicular to the easy-axis. Most of spins experience about 120 Oe field. Bottom: The perpendicular field for most of spins that experience a small (< 5 Oe) parallel field is also close to zero.

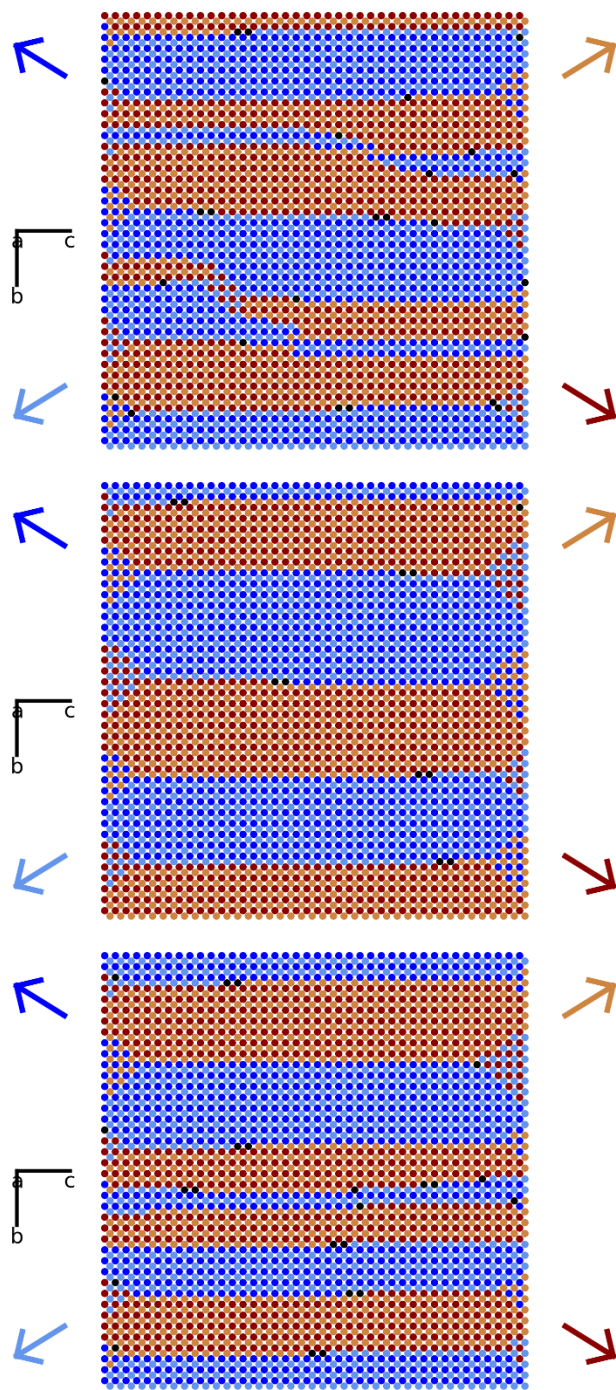


Figure S22. Magnetic structure obtained by Monte Carlo simulations of magnetic moments in **1**. Top: sample 2, middle: sample 3, bottom: sample 4. The view is along the 100 axis, i.e. along the Co chains. Two possible easy axes directions are marked by arrows. Each dot denotes a single chain of spins. The orientation of magnetic moments is marked by colors. Black dots denote chains that reverse by applied field of $H_{ac} < 5$ Oe.

References for SI:

- [S1] J. Werner, M. Rams, Z. Tomkowicz and C. Näther; A Co(II) Thiocyanato Coordination Polymer with 4-(3-Phenylpropyl)pyridine: Influence of the co-Ligand on the Magnetic Properties, *Dalton Trans.*, **2014**, *43*, 17333–17342.
- [S2] J. A. Quilliam, L. R. Yaraskavitch, H. A. Dabkowska, B. D. Gaulin, J. B. Kycia; Dynamics of the magnetic susceptibility deep in the Coulomb phase of the dipolar spin ice material $\text{Ho}_2\text{Ti}_2\text{O}_7$, *Phys. Rev. B*, **2011**, *83*, 094424.
- [S3] H. A. Farach, R. J. Creswick, C. P. Poole; *Superconductivity*, Academic Press, San Diego **1995**.
- [S4] Cole K. S., Cole R. H. Dispersion and Absorption in Dielectrics I. Alternating Current Characteristics, *J. Chem. Phys.*, **1941**, *9*, 341 – 351.